Microgrid modular design for Tribal Healthcare facilities: Kayenta Health Center PV system case study

Samuel Vega Cotto
Student Member IEEE
University of Texas in Arlington / Indian Health Service
Dallas, TX USA
Samuel.Vega-Cotto@ihs.gov

Wei-Jen Lee
Fellow IEEE
University of Texas in Arlington
Arlington, TX USA
wlee@uta.edu

***Abstract*—This paper describes an experimental process and detailed information related to an 100KW PV system case study at the Kayenta Health Center, which is located in the Navajo Nation. Information about the solar irradiance on site, the PV system performance, the power quality at the facility, and observation of the related equipment is gathered. Experimental data validate the theoretical data available for the zone, the facility, the systems and the equipment. Detailed study of existing PV system at the Navajo nation combined with modeling and simulation will discover additional information, tools, process and methodology for the future implementation of the microgrid in other tribal health care facilities. Observation and results demonstrate that the actual implementation of the microgrid at Kayenta Health Center enhance the power quality, result in optimum power system design, produce energy savings and reduce environmental pollution.**

Keywords—Microgrid; tribal healthcare facilities; renewable energy; PV systems; Indian Health Services; experimental, Kayenta

I. INTRODUCTION

The Indian Health Service (IHS) in considering a power system design around the Microgrid concept for existing or new healthcare facilities in order to improve flexibility, reliability and energy savings. Kayenta Health Center is a new hospital that began operations in July 2016. The power system at Kayenta HC is over designed, very stiff and traditional. The study of the PV system performance and the electrical load behavior is important to evaluate the possibility of expanding renewable energy components. This paper describes the experimental process performed at the Kayenta HC, which focused on a detailed study of the PV system and is complemented with additional examination of the Power Quality at the facility. During the latest stage of construction, the power system at Kayenta HC has been experiencing a significant number of power disturbance events, which result in operational inconvenient.

Navajo Tribal Utility Authority (NTUA) provided two separate feeders, each one connected to a 2.5MVA, 25KV - 480/277V transformer. Each transformer feeds one side of double-ended switchgear (3000A, 480/277V). The system provides redundancy of main feeder and transformer. However, the power source comes from the same substation.

The Indian Health Service, Office of Environmental Health and Engineering, Division of Engineering Services supports this work.

The PV system consists of Suniva optimus monocrystalline solar modules (model OPT # 265-60-4-100). There are 378 modules installed in two different roof areas of the facility. The inverter is Solectria Renewables, model PVI 100KW, 480V. The inverter output is connected to the double-ended switchgear.

Five (5) diesel generators (1000KVA @ 0.8PF, 480/277V) provide emergency power for the entire facility in case of loss of power or power quality issues from the utility. The emergency power supply system (EPSS) also includes three main automatic transfer switches (ATS) to separate the loads into the different categories for healthcare facilities: critical, life safety and equipment branches [1].

II. EXPERIMENTAL PROCESS

A. Proposed Strategy

The main purpose of this study was to gather actual and useful information about the existing PV system installed in the Kayenta HC. A secondary goal was to observe and verify the Power Quality of the electrical service received from the NTUA. The study of the PV system was based mainly on four different tasks. First, installation of a Power Logger in the output of the inverter and get real time performance for an entire week (see Fig. 1). Second, use a light meter to obtain sample readings of actual light intensity to be converted to solar irradiance data. Third, use a Multimeter to obtain sample readings of voltage and current on a timely basis of the input and output of the inverter. Fourth, field visual observation and/or measurements for the different components of the PV system. In order to study the Power Quality of the NTUA electrical service, a Power Quality and Revenue meter was installed in the main breaker of the SES-2 side of the double-ended switchgear (see Fig. 2).

Fig. 1. Power Logger (Fluke 1735) installed in the output of the Inverter

Other actions or tasks were included or modified based on observation of the system in the field.

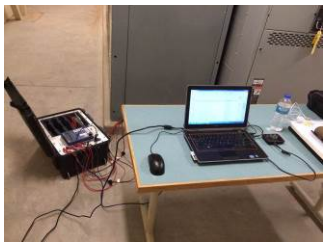

Fig. 2. Power Quality & Revenue Meter (SEL 735) installed in SES-2

B. *PV System performance*

A Power Logger was used to monitor the PV system performance at the Kayenta HC. The Power Logger can conduct voltage, current and power measurement to determine existing loads. The Logger is also a general-purpose power quality investigative tool that reveals the quality of voltage supply at any point in a distribution network [4]. The sampling time was preset to every five minutes to be able to record an entire week or more of PV system performance without interruption.

Fig. 3 and Fig. 4 illustrate the power and energy recorded during one week for the PV system. The reactive power is insignificant compared with the real power, such that the apparent power is almost equivalent to the real power. The graph shows minimum, maximum and average values. The period of performance is from July 26, 5:13PM until August 2, 8:03AM. During this week, there were variances in the weather conditions reflected in the performance of the system. It can be noticed from the graph, some variances in the power and energy due to clouds and rain especially during the days July 30, July 31, August 1, and August 2. July 27 was a perfect sunny day and July 29 was mostly sunny. On July 28, about 12:45PM until 2PM the graph shows a power interruption. This interruption was due to simulation of a utility power outage (opening SES-2 main breaker) while exercising and testing the emergency generators.

C. *Power Quality of NTUA*

The main purpose of using power quality meter is to verify the events (voltage sag/swell/interruption, VSSI) perceived at the facility. The service unit personnel reported an average of two voltage interruptions every week. The events cause the Chillers and Air Handling Units (AHU) to shut down and the building management system could not handle automatic recovery. It was observed that at least three external events triggered the emergency generators requiring service unit personnel to take action and manually restart the HVAC equipment during the same week. Tripping of HVAC equipment due to voltage sags can be prevented in most instances by the use of a Static Transfer Switch (STS) [9]. Applying the STS reduce the total duration of a voltage out-of-specifications to approximately 1/8 cycle and the current out-of-specifications to approximately 1/4 cycle [10].

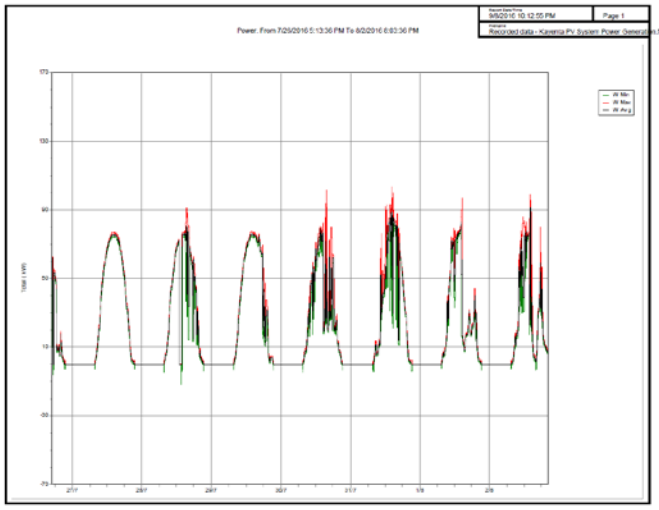

Fig. 3. Power Delivered by PV system at Kayenta HC – one week

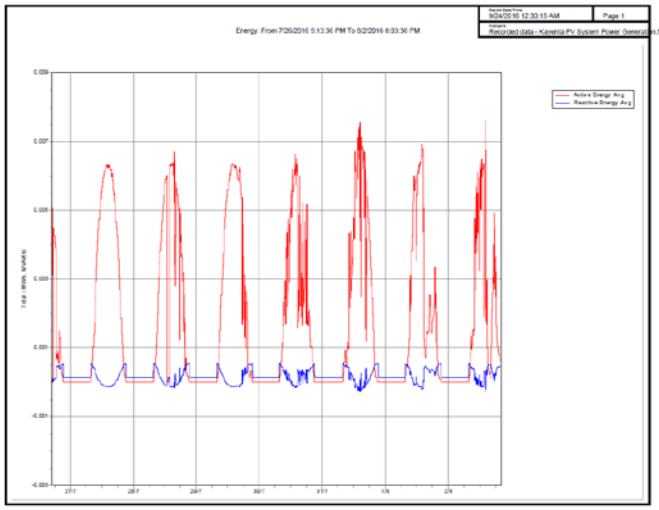

Fig. 4. Energy supplied by PV system at Kayenta HC – one week

The settings of the power quality meter were verified to match IEEE STD 1159 - Recommended Practice for Monitoring Electric Power Quality. Table 1 shows events recorded by the power quality meter. Recorded events include swells, momentary interruption and sustained interruptions.

The average values of Total Current Harmonic Distortion (THD) are around 30% for A, B and C phases and 50% for Neutral. The fluctuation ranges of THD currents for phases A, B, C and N respectively are 25% to 35%, 20% to 35%, 25% to 35% and 30% to 75%. Due to this observation, it was decided during the experimental process to connect the Power Logger for 24 hours to the critical load branch in order to compare with the overall THD of the facility electrical system.

TABLE I

EVENTS (VSSI) RECORDED BY POWER QUALITY & REVENUE METER

FileType	Version	Date	Time	ChartField	TimeSource
VSSI	5.17.0.2	09/29/16	21:13:39.212	#	Internal
RecNum	Date	Time	Phase	Status	
-1	1	2	14	15	
Ia	Ib	Ic	Ig	In	Vbase-a
3	4	5	6	7	8
DeviceID	FID	TID	NOMINAL_ABCG	NOMINAL_N	VBASE
KAYENTA	"SEL-735-R115-V4-Z008005-D20151217"	"MAIN SWITCHGEAR"	5	5	120
Event	Date	Time	Duration	Type	Magnitude
#0001	07/26/2016	16:21:47.381	000:00:00.014	SWELL	162.6
#0002	07/26/2016	16:21:47.381	000:00:16.571	POWERLOSS	0
#0003	08/02/2016	15:05:56.329	000:00:00.046	SWELL	246.3
#0004	08/02/2016	15:06:15.210	000:01:11.273	POWERLOSS	0
#0005	08/03/2016	15:23:32.603	000:00:00.029	SWELL	246.8
#0006	08/03/2016	15:23:32.603	000:01:11.277	POWERLOSS	0
#0007	08/04/2016	16:22:38.676	000:00:16.313	POWERLOSS	0

D. Field Observations

On July 27, dirt was observed on the surface of the PV modules. The dirt is considered a factor in the overall performance of the system, since it behaves like a partial shadow, avoiding the full solar irradiation of the PV cells. Cleaning of all the PV modules was coordinated and performed on July 29.

A PV module glass was impacted during a hailstorm that occurred a few months before the experimental process. The performance of this module was questionable, such that additional voltage and current measurements were necessary. Based on these measurements, it was verified that the PV module had an acceptable performance even with the glass damaged.

III. DATA ANALYSIS

A. Irradiance data

The light meter was used to take manual readings of the daylight. Daylight, or the light of day, is the combination of all direct and indirect sunlight during the daytime. The brightest sunlight is 120,000 lux for direct sunlight [2]. At Earth's average distance from the Sun (about 150 million kilometers), the average intensity of solar energy reaching the top of the atmosphere directly facing the Sun is about 1,360 watts per square meter, according to measurements made by the most recent NASA satellite missions [3]. After deep analysis of the data, it was observed that the daylight measurements and theoretical irradiance curves have the same shape and are proportional. Based on the above facts and findings, the daylight readings can be normalized to obtain approximate values of actual irradiance. These values are compared with historical values listed in the National Renewable Energy Laboratory (NREL).

Sample readings of the daylight were taken on different days. On July 28, the readings were taken from sunrise to sunset with time intervals of approximately ten (10) minutes. Hence, this data was selected for comparison. These are instantaneous readings at a specific time during the day, so further conversion is needed to match the historical data from the NREL, which is in Wh/m^2.

Nearly all of the solar data in the National Solar Radiation Database (NSRDB) are modeled, and only 40 sites have measured solar data—none of them with a complete period of record [5]. Hence, it is important to be able to compare actual data with the historical data from NSRDB. According to [5], the hourly extraterrestrial radiation on a horizontal surface is equal to the amount of solar radiation received on a horizontal surface at the top of the atmosphere during the 60-minute period ending at the timestamp. Based on this definition, the hourly extraterrestrial radiation can be obtained by properly averaging the irradiance over one-hour periods.

Solar irradiance data corresponding to July 28 was analyzed and tested with various methods of conversion including linear interpolation, smoothing data using Gaussian Kernel, smoothing data with a median smoother and smoothing data using an adaptive method. The smoothing data using an adaptive method was selected as it shows better results for this application. Fig. 5 shows the results of applying this method. Notice the effect of smoothing the shape of the curve.

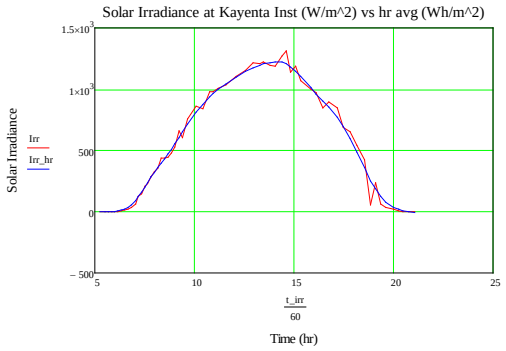

Fig. 5. Solar Irradiance at Kayenta, Instantaneous vs hourly average

Finally, the actual data obtained, derived in the procedure and shown in Fig. 5, is compared to the historical data from the NSRDB. It is important to point out that the data available at the NSRDB is from Flagstaff, which is located 150 miles southwest of Kayenta.

Fig. 6 shows the results for this procedure. Notice that the actual solar irradiance data is approximately equal to the historical solar irradiance data in the zone. The PV modules at Kayenta are mounted on ENRGY Curb TPO 10-01, which provides for fixed tilt at ten degrees, and modules are oriented to the south. It has been proved that there is a correlation between the orientation, tilt, tracking and the solar photovoltaic output [11]. The actual solar irradiance curve observed in Fig. 6 matches the magnitude and the shape mostly in the second half.

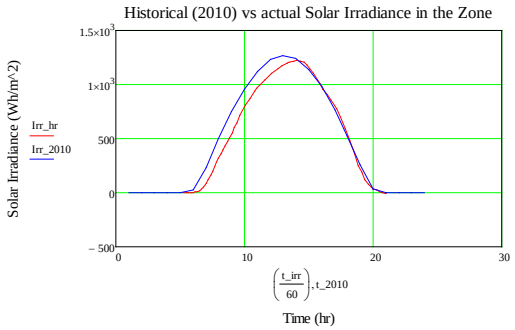

Fig. 6. Historical (2010) vs actual Solar Irradiance in the zone

However, this method was applied to the data collected on August 1 and it was proven that it is not useful for cloudy days. Because of the data-filling methods used to accomplish the goal of serial completeness for the solar data, NSRDB meteorological data may not be suitable for climatological work. NSRDB-modeled data may introduce unexpected errors if used for applications that require accurate hourly tracking of true solar irradiance, such as photovoltaic system performance analyses [5].

B. PV System data

The dirtiness effect can be measure by comparison of the PV system performance before and after the cleaning of the PV modules. However, it is also necessary to consider in the measurements that the PV performance is proportional to the solar irradiance. The historical solar irradiance covering the period represented before and after the cleaning is essentially the same for each day. Hence, in this particular case, it is only necessary to evaluate the power output performance before and after the cleaning of the PV modules. Although the shape of the curve is somewhat distorted due to the clouds on July 30 and 31, some improvement of the maximum power output in Fig. 7 can be observed. The difference in the average maximum power output before and after the cleaning is 7.5KW (82.5KW - 75KW). This implies a decrease of 9% in the PV system performance due to the dirtiness. Based on the average commercial electricity rate in the zone and the existing PV system configuration, this factor represents $1,426.00 per year of energy value [12].

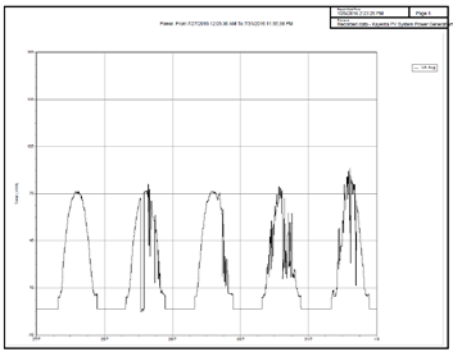

Fig. 7. Actual PV system Power Output in Kayenta July 27 to July 31

An important factor for the Microgrid and sizing the Renewable Energy components is the electrical load demand for the facility. It is also important to study the behavior of the load demand over time. Fig. 8 shows the power load profile recorded by Power Quality and Revenue meter at SES-2. Notice that the load profile data was selected to match the same period of the PV system power output from the Power Logger (Fig. 7). The power demand shown on Fig. 8 is supplied by the PV system plus the NTUA. Based on this load information, it can be determined how many additional modules can support island mode operation of the Microgrid.

A very interesting detail when comparing Fig. 7 with Fig. 8 is that the power demand increased significantly during the day, matching the time where the solar energy is available. The solar energy is obviously useful for peak shaving in this type of application. Even more interesting is the difference between cloudy and sunny days. It is obvious that the average solar power available during cloudy days is lower. Nevertheless, notice the peak demand during sunny days (245KVA, 275KVA, 260KVA) is higher than the peak demand during cloudy days (210KVA, 190KVA). The reason for this is that the higher electrical load in the facility are the Chillers, which operates lightly at lower temperatures during cloudy or rainy days. This is good for the usefulness of the solar power. However, this effect occurs during summer time and further study is necessary during the winter. In addition, there is a power demand average of about 120KVA during nighttime.

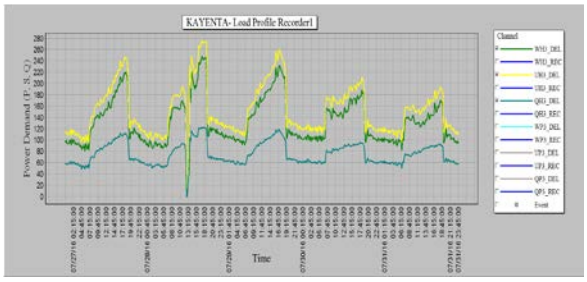

Fig. 8. Power Load profile at SES-2, July 27 to July 31

A useful tool for planning the PV system resources including the effect of meteorological analysis is available via an interactive web platform in www.renewables.ninja. Fig. 9 shows simulated power output performance for the existing PV system in the Kayenta HC from July 27, 2014 to July 31, 2014. On average, the simulated performance is approximate to the actual performance shown in Fig. 7, although some variations can be noticed on July 28.

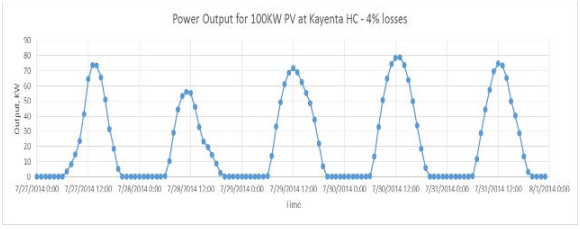

Fig. 9. Power Output - PV system at Kayenta 7/27/14 to 7/31/14: source www.renewables.ninja

C. Inverter Efficiency data

During August 1 to August 2, sample measurements were obtained of voltage and current on a timely basis in the input and output of the inverter. The record of field measurements and the corresponding calculations demonstrated an average efficiency of 96.17%. According to the manufacturer, the inverter peak efficiency is 96.9%, while the average efficiency (California Energy Commission weighted efficiency) is 96.5% [18]. Therefore, it can be stated that the PV system losses within the inverter are almost 4%.

D. Power Quality data

Most of the VSSI can be prevented in most instances by the use of STS. Fig. 10 illustrates a block diagram of modification for existing power system. It suggests additional components of PV systems, wind turbine systems or even reconnection of existing diesel generators to a new Microgrid panel that would be connected to the STS. In grid-connected mode, the renewable energy components are connected to SES-2 through the STS. In

islanded mode, the renewable energy components are connected and synchronized to the emergency switchboard. The configuration would maximize the use of renewable energy during extended operation in islanded mode. Notice that proper power sensing and control system needs to be applied for the correct operation of the STS.

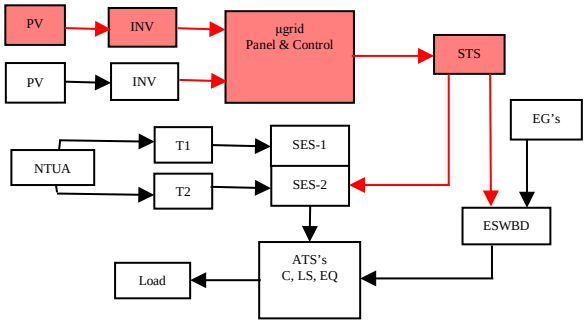

Fig. 10. Block diagram of modified configuration of existing power system, Kayenta HC

The load profile #2 (LDP2) of the Power Quality and Revenue meter records aggregated voltage, current, imbalance, and THD at three (3) second intervals [19]. The voltage per phase averaged 2.89% (285V) over the nominal value (277V) and it behaves steadily, although some VSSI from the NTUA were registered. Fig. 11 shows the current level performance.

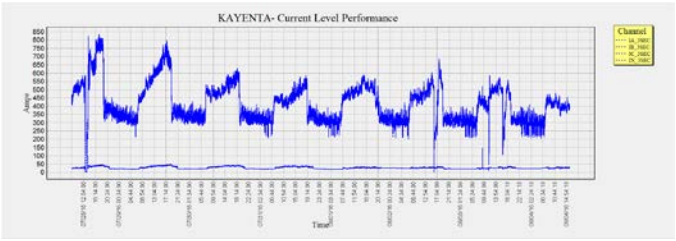

Fig. 11. Current level performance, Kayenta HC

E. Harmonics

The Power Quality and Revenue meter displayed high content of harmonic currents, although the harmonic voltages were shown to be very low. The Power Logger was connected to the critical loads during 24 hours, while the Power Quality and Revenue meter remained in the main breaker (SES-2).

Total Harmonic Distortion (THD) current average values are 28.2%, 27%, 30.2%, 50.4% for A, B, C and N respectively. The maximum values of THD currents for phases A, B, C and N respectively are 35.8%, 35.3%, 48.2% and 91.2%. Fig. 12 shows the THD current values measured at three (3) second intervals from August 1 to August 4. The THD current values (average and maximum) for the selected 24-hour period were very close to the values for the entire period. Fig. 13 show the THD current values measured to the critical loads branch. The THD current average values are 14.0%, 12.5%, 14.9%, 26.6% for A, B, C and N respectively. It is not clear how these THD values at the critical branch can relate to the THD values at SES-2, but some calculations can be done with the information available. The THD is a measure of the effective value of the harmonic components of a distorted waveform [20]. This index for current can be calculated:

$$THD = \frac{\sqrt{\sum_{h=2}^{n} I_h^2}}{I_1} \qquad (1)$$

Where I_h is the rms value of harmonic component h of the current. The THD is related to the rms value of the current as follows:

$$I_{rms} = I_1 * \sqrt{1 + THD^2} \quad or \quad I_1 = \frac{I_{rms}}{\sqrt{1 + THD^2}} \qquad (2)$$

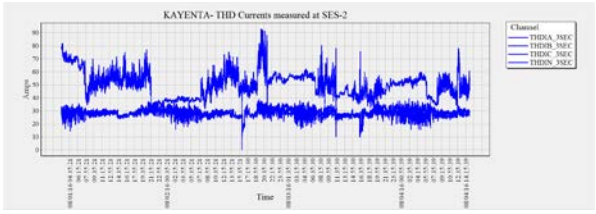

Fig. 12. THD Currents performance, at SES-2

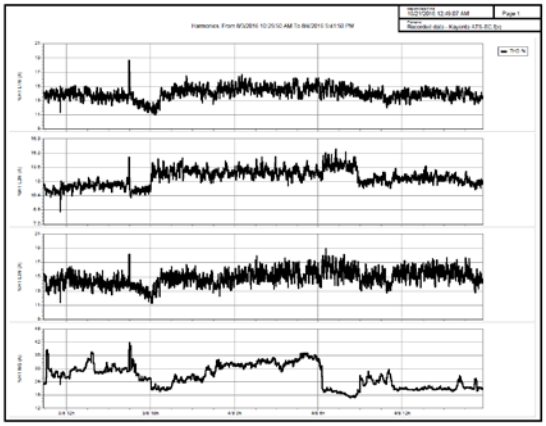

Fig. 13. THD Currents performance, at Critical loads branch

The average rms currents and average THD are obtained from the data measured with the instruments as shown in Fig. 14. Hence, the average fundamental component of the currents is obtained applying (2). By KCL, the average rms currents and average fundamental components of the currents can be obtained for the combination of LS and EQ branches. Hence, rearranging (2) obtain the THD for the combination of LS and EQ branches.

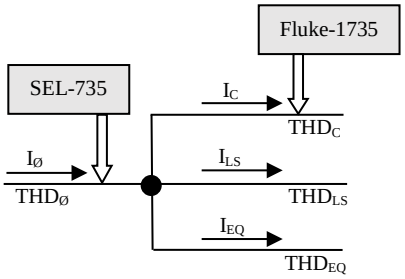

Fig. 14. KCL for THD Calculations

IEEE Standard 519-2014 refers THD to the fundamental of the peak demand load current rather than the fundamental of the

present sample. This is called total demand distortion and is given by:

$$TDD = \frac{\sqrt{\sum_{h=2}^{n} I_h^2}}{I_L} = \frac{THD * I_1}{I_L} \qquad (3)$$

Where I_L is the peak demand load current at the fundamental frequency component measured at the point of common coupling (PCC) [20]. The Power Quality and Revenue meter recorded the peak demand currents for each phase and the neutral. Table 2 shows a summary of the results. The THD of the critical branch is slightly less than half of the THD of the combined LS and EQ branches for A, B and C phases and one-third for N. Most of the harmonic currents are produced in the combined LS and EQ branches, but which one produces more? By observation in the field, LS is the lighter load and EQ is the heavier load of all three branches. Since the THD refers to the fundamental of the present sample in each branch, without taking additional measurements, it can be concluded that most of the harmonic currents are produced in the equipment branch.

TABLE II

SUMMARY OF HARMONIC CURRENT MEASUREMENTS AND CALCULATIONS

	SES-2				Critical branch				Combined LS and EQ branches			
Phase	A	B	C	N	A	B	C	N	A	B	C	N
I1 (A)	368.6	370.4	355.7	23.0	71.5	60.3	52.1	15.1	297.1	310.1	303.6	8.0
Irms (A)	383	383.7	371.6	25.8	72.2	60.8	52.7	15.6	310.8	322.9	318.9	10.2
THD (%)	28.2	27.0	30.2	50.4	14.0	12.5	14.9	26.6	30.7	29.0	32.1	80.0
TDD (%)	12.7	12.6	13.0	22.8								

IEEE standard 519-2014 establishes current distortion limits for systems rated 120V through 69kV [23]. These limits increase as the ratio of I_{SC} / I_L increases, where I_{SC} is the maximum short-circuit current at PCC. I_{SC} is provided in the submittal for the short circuit and device coordination study for new healthcare facilities. Calculations show $20 < I_{SC}/I_L = 45.2 < 50$ and recommends a limit of TDD = 8.0. It is important to notice that the Kayenta HC is a single load in a remote location connected to an isolated feeder of NTUA; however, some energy savings can be achieved by reducing the harmonic currents.

IV. MODELING KAYENTA PV SYSTEM

Modeling and simulation is a proven method for research and development of the PV systems [24]-[27]. The theory of PV system modeling can be combined with manufacturer datasheets of existing equipment, the data obtained experimentally and other resources in order to produce accurate simulations of different conditions and expanded systems. Literature has a lot of research regarding different techniques of Maximum Power Point Tracking (MPPT) for the control of PV systems [29]-[34]. MPPT techniques are used to increase or to maximize the output power of photovoltaic system.

A. Mathematical Model to match Kayenta PV system

The existing PV system in Kayenta can be modeled using the ideal single-diode model (ISDM) approach, which is represented with a circuit composed of an ideal current source in parallel with an ideal diode [28]. The ISDM takes advantage of the simplicity of ideal models and has the capability of extracting accurate estimates of the model parameters, directly related to manufacturer datasheets. A complete nomenclature and description of equations is presented in [24]. Input data for the ISDM are temperature and irradiance. Temperature information is obtained from NREL historical data (during July T_{avg}=19.1°C, T_{max}=27.7°C, T_{min}=10.3°C). Solar irradiance from experimental data during a sunny day in July can be approximated with a mathematical formula,

$$E_e(t) = \left[E_{max} - \left(\frac{t}{TF} - \sqrt{E_{max}}\right)^2\right] \frac{W}{m^2} \qquad (4)$$

Where E_{max} is the typical maximum irradiance during a day in July and TF is a time factor to adjust the data over the daylight period. Notice the irradiance is a function of time during the day.

Parameters obtained from the datasheet (Suniva Optimus OPT #265-60-4-100) are: the PV-cell temperature at STC, Irradiation at STC, PV open-circuit voltage at STC, PV short-circuit current at STC, PV voltage at the maximum power point, PV current at the maximum power point of STC, Temperature coefficient on PV current, and Temperature coefficient on PV voltage. The diode ideality factor A can be calculated from the equation,

$$\frac{e^{\left(\frac{q*V_{MPP}}{k*A*T_{CS}}\right)} - 1}{e^{\left(\frac{q*V_{OCS}}{k*A*T_{CS}}\right)} - 1} = 1 - \frac{I_{MPP}}{I_{SCS}} \qquad (5)$$

The diode reverse bias saturation current (I_{SS}) is calculated and can be used to reproduce the PV cell solar module I-V characteristic and the power characteristic for verification against the datasheet. The PV photon current changes with solar irradiation and cell temperature. Keeping the change in temperature constant and applying (4) for the solar irradiance, the PV photon current is expressed as a function of time during the day.

$$i_{ph}(t, \Delta T) = \frac{E_e(t)}{E_{STC}} * I_{SCS} * (1 + \alpha_T * \Delta T) \qquad (6)$$

The updated I-V characteristic equation can be written as a function of time during the day,

$$i_{PV}(t, \Delta T) = i_{ph}(t, \Delta T) - i_S(\Delta E_e(t), \Delta T) * \left[e^{\left(\frac{q*V_{PV}}{k*A_v*(T_{CS}+\Delta T)}\right)} - 1\right] \qquad (7)$$

Where $\Delta E_e(t) = E_e(t) - E_e(t\text{-}1)$ monitor the change in irradiance during minor periods and the value of v_{PV} is determined by the balance between the PV generation and the load. The shape and size of the load can also be represented mathematically as a function of time during the day using experimental data shown in Fig. 8.

B. Simulation expanded Kayenta PV system in Simulink

Simulink is a widely use tool for modeling and simulation of different MPPT techniques [30]-[33]. Among the different MPPT techniques are Fractional Short Circuit Current (FSCC), Fractional Open Circuit Voltage (FOCV), Perturb & Observe

(P&O) and Incremental Conductance (IC). The Simulink library browser contains some examples of renewable energy models, which apply MPPT techniques [35]. By taking advantage of the MPPT P&O technique, a model was configured to match an expanded system as shown in the block diagram of Fig. 10.

The model is shown in Fig. 15. The PV array is represented with 81 parallel strings. Each string has 14 Suniva Optimus OPT #265-60-4-100 modules connected in series. This is equivalent to adding two additional modular systems equal to the existing one (100kW) for a total of 300kW. The PV array block has two inputs that allows varying sun irradiance and temperature. The three-phase inverter is modeled using a 3-level IGBT bridge PWM-controlled. This component represents three 100kW inverters. A 300-kVA, 227V/480V three-phase transformer and STS are used to connect the inverter to the bus bar at SES-2. The facility load shown in Fig. 8 is represented by the 300 kW load and the existing transformer that connects NTUA is 2.5MVA, 25kV/480V. The grid modeled is typical in the zone.

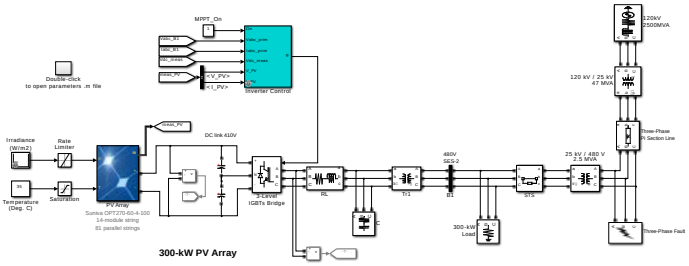

Fig. 15. Expanded PV System model for Kayenta HC

C. Simulation Results

Several simulations were performed with the model. As a worst-case scenario, a three-phase fault was simulated very close to the facility. The initial input irradiance to the PV array model is 1000 W/m^2 and the operating temperature is 35°C. PV voltage (Vdc_mean) of 418 V and the power extracted (Pdc_mean) from the array is 294 kW are close to the expected values from the PV module manufacturer specifications. From t=0.3 sec to t=0.7, the solar irradiance changed from 1000 W/m^2 to 200 W/m^2. From t=1 sec to t=1.5 sec, a three phase fault is introduced. However, the STS disconnects the NTUA side in 1/4 cycle and the system quickly clears the fault by switching to islanded mode.

V. Conclusion

Experimental studies performed on site at the Kayenta HC provided useful information about the actual solar irradiance in the zone, the existing PV system, Inverter efficiency, Power Quality of NTUA and Harmonics. A method to approximate solar irradiance from manual readings of the daylight was presented. Results proved that existing historical solar irradiance data in the zone and power output obtained from web platform in www.renewables.ninja are useful tools for planning the PV system resources for the Microgrid in tribal healthcare facilities. The difference in the average maximum power output performance due to the dirtiness implies a decrease of 9%. Power demand increases significantly during the day, matching the time where the solar energy is available. Peak demand during sunny days is higher than the peak demand during cloudy days because the Chillers operate lightly at lower temperatures during cloudy or rainy days.

Most of the VSSI recorded can be prevented in most instances by the use of a STS. STS application together with the design around the Microgrid concept can be considered for new tribal healthcare facilities in the zone. By strategically collocating the Fluke 735 during 24 hours in one of the three branches of the healthcare facility combined with some calculations, it was determined that most of the harmonic currents are produced in the equipment branch.

Theoretical equations were combined with experimental solar irradiance data and historical temperatures in order to produce a more accurate mathematical representation of the existing PV system. A Simulink model was used to study the interaction between a proposed expanded PV system with the existing power system around the Microgrid concept.

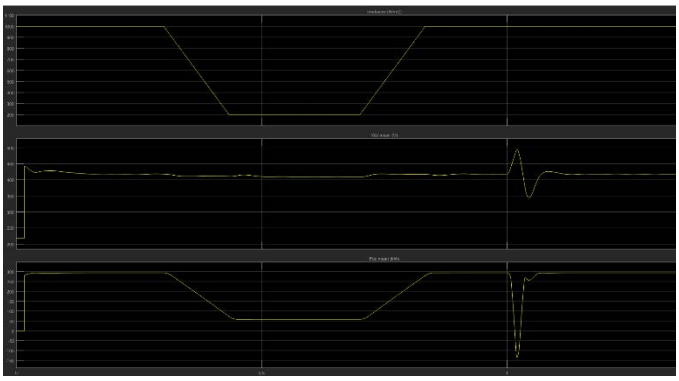

Fig. 16. Simulation results DC side - Expanded PV System model for Kayenta HC

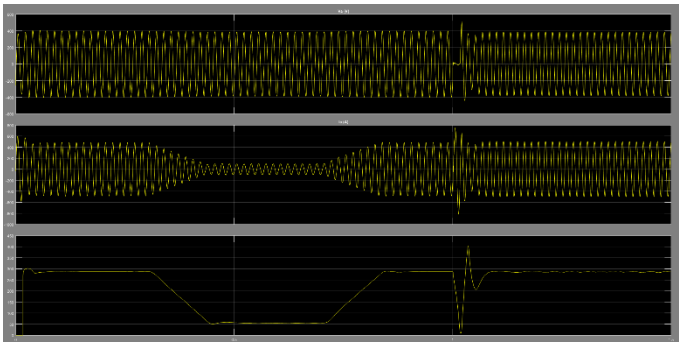

Fig. 17. Simulation results AC side - Expanded PV System model for Kayenta HC

Acknowledgment

These research efforts are supported by the Indian Health Service, Office of Environmental Health and Engineering, Division of Engineering Services.

References

[1] Samuel Vega-Cotto, Wei-Jen Lee, “Challenges and opportunities: Microgrid modular design for Tribal Healthcare facilities”, 2016 North American Power Symposium (NAPS), Denver, CO, 2016, pp. 1-6.

[2] Wikipedia [Online]. Available: https://en.wikipedia.org/wiki/Daylight

[3] NASA Earth Observatory website [Online]. Available: http://earthobservatory.nasa.gov/Features/EnergyBalance/page2.php

[4] Fluke® Corporation, "Fluke 1735 Power Logger Users Manual", March 2006 Rev. 2, 3/10

[5] Stephen Wilcox, "National Solar Radiation Database 1991–2010 Update: User's Manual," Technical Report, NREL/TP-5500-54824, August 2012

[6] National Renewable Energy Laboratory (NREL) database. [Online]. Available: http://rredc.nrel.gov/solar/

[7] SEL-735 Guideform Specification. [Online]. Available: https://selinc.com/

[8] IEEE Std 1159™-2009 - IEEE Recommended Practice for Monitoring Electric Power Quality, The Institute of Electrical and Electronics Engineers, Inc., IEEE Power & Energy Society, 26 June 2009.

[9] Phillip W. Hall, Bill B. Bailey, Ernst H. Camm, "Power Quality Evaluation at Medical Center," Transmission and Distribution Conference, 1999 IEEE, Pages: 560 - 565 vol.2.

[10] Milind M. Bhanoo, "Static Transfer Switch: Advances in High Speed Solid-State Transfer Switches for Critical Power Quality and Reliability Applications," Textile, Fiber and Film Industry Technical Conference, 1998 IEEE Annual, Pages: 5/1 - 5/8.

[11] US Energy Information Administration [Online]. Available: http://www.eia.gov/todayinenergy/detail.php?id=18871

[12] NREL's PVWatts® Calculator [Online]. Available: http://pvwatts.nrel.gov/

[13] Abd Salam AI-Ammri, Areej Ghazi, Falah Mustafa, "Dust Effects on the Performance of PV Street Light in Baghdad City," Renewable and Sustainable Energy Conference (IRSEC), 2013 International, P. 18 – 22.

[14] Adria E. Brooks; Daniella N. DellaGiustina; Scott M. Patterson; Alexander D. Cronin, "The consequence of soiling on PV system performance in Arizona; Comparing three study methods," 2013 IEEE 39th Photovoltaic Specialists Conference (PVSC), Pages: 0754 – 0758.

[15] Shaharin A. Sulaiman; Mohamad Nur Hidayat Mat; Fiseha M. Guangul; Mohammed A. Bou-Rabee, "Real-time study on the effect of dust accumulation on performance of solar PV panels in Malaysia," International Conference on Electrical and Information Technologies (ICEIT), 2015, Pages: 269 – 274.

[16] Mohammad Naeem; Govindasamy TamizhMani, "Cleaning frequency optimization for soiled photovoltaic modules," 2015 IEEE 42nd Photovoltaic Specialist Conference (PVSC), Pages: 1 – 5.

[17] Hirotoshi Nakagawa; Kouhei Mathuoka; Hironobu Yonemori, "A study about the self-cleaning of a PV module surface using photocatalyst," Humanitarian Technology Conference (R10-HTC), 2014 IEEE Region 10, Pages: 82 – 87.

[18] Yaskawa Solectria Solar, Product Datasheet & Specifications [Online] Available: https://www.solectria.com/pv-inverters/commercial-central-inverters/pvi-50-100kw/

[19] SEL-735 Portable Operating Instructions. [Online]. Available: https://selinc.com/

[20] Roger C. Dugan, Mark F. McGranaghan, Surya Santoso, H. Wayne Beaty, "Electrical Power Systems Quality 3rd Ed," McGraw-Hill 2012.

[21] Stefan Pfenninger, Iain Staffell, "Long-term patterns of European PV output using 30 years of validated hourly reanalysis and satellite data," Copyright © 2016 Elsevier B.V. or its licensors or contributors.

[22] Iain Staffell, Stefan Pfenninger, "Using bias-corrected reanalysis to simulate current and future wind power output," Copyright © 2016 Elsevier B.V. or its licensors or contributors.

[23] IEEE Std 519™-2014 - IEEE Recommended Practice and Requirements for Harmonic Control in Electric Power Systems, The Institute of Electrical and Electronics Engineers, Inc., IEEE Power & Energy Society, 27 March 2014.

[24] Weidong Xiao, Fonkwe Fongang Edwin, Giovanni Spagnuolo, Juri Jatskevich, "Efficient approaches for modeling and simulating photovoltaic power systems," IEEE journal of photovoltaics, jan 2013, vol. 3, No. 1.

[25] Jan T. Bialasiewicz, "Renewable energy systems with photovoltaic power generators: operation and modeling," IEEE transactions on industrial electronics, jul 2008, vol. 55, No. 7.

[26] P.I. Muoka, M.E. Haque, A. Gargoom, M. Negnevitsky, "Modeling, simulation and hardware implementation of a PV power plant in a distributed energy generation system," IEEE PES, 2013.

[27] Amirnaser Yazdani, Anna Rita Di Fazio, Hamidreza Ghoddami, Mario Russo, Mehrdad Kazerani, Juri Jatskevich, Kai Strunz, Sonia Leva, Juan A. Martinez, "Modeling guidelines and benchmark for power system simulation studies of three-phase single-stage photovoltaic systems," IEEE transactions on power delivery, apr 2011, vol. 26, No. 2.

[28] Yousef Mahmoud; W. Xiao; H. H. Zeineldin, "A Simple Approach to Modeling and Simulation of Photovoltaic Modules," IEEE Transactions on Sustainable Energy, Year: 2012, Volume: 3, Issue: 1, Pages: 185 – 186.

[29] Moacyr A. G. de Brito; Leonardo P. Sampaio; G. Luigi; Guilherme A. e Melo; Carlos A. Canesin, "Comparative analysis of MPPT techniques for PV applications," 2011 International Conference on Clean Electrical Power (ICCEP), Pages: 99 – 104.

[30] Ali F Murtaza; Hadeed Ahmed Sher; Marcello Chiaberge; Diego Boero; Mirko De Giuseppe; Khaled E Addoweesh, "Comparative analysis of maximum power point tracking techniques for PV applications," 2013 16th International Multi Topic Conference (INMIC), Pages: 83 – 88.

[31] Soubhagya Kumar Dash; Deepak Verma; Savita Nema; R. K. Nema, "Comparative analysis of maximum power point (MPP) tracking techniques for solar PV application using MATLAB simulink," 2014 Recent Advances and Innovations in Engineering (ICRAIE), Pag.: 1 – 7.

[32] R. Boukenoui; R. Bradai; A. Mellit; M. Ghanes; H. Salhi, "Comparative analysis of P&O, modified hill climbing-FLC, and adaptive P&O-FLC MPPTs for microgrid standalone PV system," 2015 International Conference on Renewable Energy Research and Applications (ICRERA), Pages: 1095 – 1099.

[33] Babita Panda; Bhagabat Panda; P. K. Hota; Sujit Kumar Bhuyan, "A comparative analysis of Maximum Power Point techniques for photovoltaic system," 2015 IEEE Power, Communication and Information Technology Conference (PCITC), Pages: 732 – 737.

[34] Abhishek Kumar Gupta; Ravi Saxena, "Review on widely-used MPPT techniques for PV applications," 2016 International Conference on Innovation and Challenges in Cyber Security (ICICCS-INBUSH), Pages: 270 – 273.

[35] Matlab & Simulink student version [Online]. Available: https://www.mathworks.com/academia/student_version/